3D Printing for Intelligent Metallic Structures

Maria Strantza, Dieter De Baere, Marleen Rombouts, Stijn Clijsters, Isabelle Vandendael, Herman Terryn, Patrick Guillaume, Danny Van Hemelrijck

7th European Workshop on Structural Health Monitoring
July 8-11, 2014. La Cité, Nantes, France

3D PRINTING FOR INTELLIGENT METALLIC STRUCTURES

M. Strantza[1], D. De Baere[2], M. Rombouts[3], S. Clijsters[4], I. Vandendael[5], H. Terryn[5], P.Guillaume[2], D. Van Hemelrijck[1]

[1] *Department of Mechanics of Materials and Constructions, Vrije Universiteit Brussel, B-1050 Brussels, Belgium*
[2] *Department of Mechanical Engineering, Vrije Universiteit Brussel, B-1050 Brussels, Belgium*
[3] *VITO Vlaamse Instelling voor Technologisch Onderzoek, Boeretang 200,2400 Mol, Belgium*
[4] *Department of Mechanical Engineering, KULeuven, Oude Markt 13, Belgium*
[5] *Department of Materials and Chemistry, Vrije Universiteit Brussel, B-1050 Brussels, Belgium*

maria.strantza@vub.ac.be

ABSTRACT

Structural Health Monitoring (SHM) is needed both to improve life-safety and to reduce the direct operational costs. Nowadays, a new concept called effective Structural Health Monitoring (eSHM) has proven to be efficient but still needs to pass different technological readiness levels to enable its implementation. This work demonstrates the feasibility study of eSHM systems produced by 3D printing or additive manufacturing. The objective of this work is to prove that the eSHM system has reached technological readiness level 3 (TRL3) and to indicate that during fatigue the integrated system has no influence on the crack initiation behaviour. First, two different techniques (selective laser melting and laser metal deposition) were used for the production of four-point bending feasibility test specimens with the integrated eSHM system. Next, a four-point bending test was selected; the specimens were subjected to the so-called step test method with constant fatigue stress amplitude and a constant R ratio. The fatigue behaviour of stainless steel and titanium alloy was studied with emphasis on crack initiation and detection. This study proves that the eSHM reaches the TRL3. The investigated system always detected cracks although further investigation is needed since higher TRL are required and the detection capability can be improved.

KEYWORDS : *structural health monitoring, pressure, additive manufacturing, fatigue, smart structure.*

INTRODUCTION

For aerospace, civil and mechanical engineering structures implementing damage detection is mandatory to improve life-safety and to reduce the direct operational costs. This process is referred to as structural health monitoring (SHM) [1]. The maturity of the different SHM systems is expressed in technological readiness levels (TRL) by the industry (e.g. Airbus) and governmental research organisation (e.g. NASA). The definition can vary for the different organisations but the main idea remains similar. A detailed review of the different TRL levels can be found elsewhere [2].

The research of effective SHM systems is resulting from the need for life-safety and the reduction of the direct operational costs. A new concept, the so-called effective structural health monitoring (eSHM) system has the intrinsic capability to accomplish the specified requirements but still needs to pass the different TRL levels to enable an implementation. The eSHM system is produced by 3D printing or additive manufacturing. Additive Manufacturing (AM) is a "process of joining materials to make objects from 3D model data, usually layer upon layer, as opposed to subtractive manufacturing methodologies", as defined by ASTM International F42 committee on

Additive Manufacturing Technologies [3]. Different AM technologies exist for the production of the materials [4]. They differ in the way layers are built to create parts, and the materials that can be used. Some methods are using melting to create the layers, whereas others methods are laying liquid materials that are cured with different technologies [5]. For the production of metal parts there are also a lot of technologies like Selective Laser Melting (SLM) [6] and Laser Metal Deposition (LMD) [7]. Both AM processes use the energy of a laser beam to bind powder particles to each other in a layer-wise manner providing full melting.

Fatigue is one of the damage phenomena that can affect the structural integrity of a metallic structural component. Microcracks typically initiate at the outer surface of the material, also in unnotched specimens with a nominally homogeneous stress distribution tested under cyclic tension. The restrain on cyclic slip is lower at the outer surface compared to the inside of the material because of the free surface at one side of the surface material. It is concluded that fatigue crack initiation is a surface phenomenon [8]. In this study, the step method was deemed a suitable method and it can provide an endurance stress for particular stress ratio with a single specimen as well as a method of generating endurance limits for one-of-a-kind specimens [9].

The objective of this study is to demonstrate the scientific feasibility (TRL 3) of the SHM concept for samples produced by LMD and SLM under laboratory controlled conditions. During this study the analytical and experimental functioning will be verified and the scientific feasibility will be fully demonstrated as TRL3 requires. This implies to prove that fatigue cracks can be detected with the capillary network and to indicate that the integrated SHM system has no significant impact on the crack initiation behaviour and location.

1. EFFECTIVE STRUCTURAL HEALTH MONITORING APPROACH

The basic physical principle of the eSHM system is checking the absolute fluid pressure changes in a 3D-curved network of capillaries or cavities that are integrated with additive manufacturing techniques in the interior of a part made with AM techniques or integrated on a standard machined part. A pressure change in the capillary indicates the presence of a crack. The 3D schematic representation of the four point bending test specimens is presented in Figure 2.

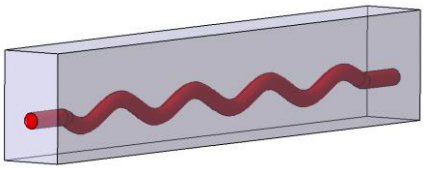

Figure 1: 3D schematic representation of eSHM system with integrated sinusoidal hollow channel

At first sight, this it is a very straightforward and robust approach to monitor the appearance of a crack; the measurement principle has already been used in the past for straight elongated capillaries [10]. A first asset of this damage identification approach is that the inspection of a complete zone can be done with one sensor at a single point on the component. A second asset is that the damage identification can be done with sensors that are available off the shelf and have already proven industrial robustness.

The practical implementation of this eSHM system, which requires the integration of internal curved capillaries/cavities in the structure, is challenging from a production as well as from a structural integrity point of view. Laser-based AM technologies like SLM and LMD are promising technologies that show potential to implement eSHM systems for fatigue crack detection. In this paper, stainless steel AISI 316L and Ti6Al4V parts with integrated capillaries are manufactured using respectively the LMD and SLM technologies. The fatigue behaviour of both materials is investigated with a four-bending test, with special attention for the crack initiation and detection. The latter are investigated through analysis of the fracture surfaces with a scanning electron

microscope. During the fatigue tests, the specimens are subjected to the step method with constant fatigue stress amplitude and a constant R ratio in each step.

2. EXPERIMENTAL STUDY

2.1 Materials and Production

Since one of the main scientific objectives of the test was to indicate that the capillary had no significant impact on the fatigue initiation behaviour of the test specimen, a 3D sinusoidal shape of the capillary was added to support this characteristic. The integrated capillary for the LMD SS316L samples has a diameter of 3mm, sinusoidal shape with amplitude of 2mm and a period of 25.7mm. On the other hand, the integrated capillary for the SLM Ti6Al4V samples has a diameter of 1mm, sinusoidal shape with amplitude of 2mm and a period of 25mm. After LMD and SLM the specimens were milled to final dimensions as specified in Figure 2. The static tensile properties for the LMD AISI 316L material and SLM Ti6Al4V are presented in Table 1 and 2 respectively.

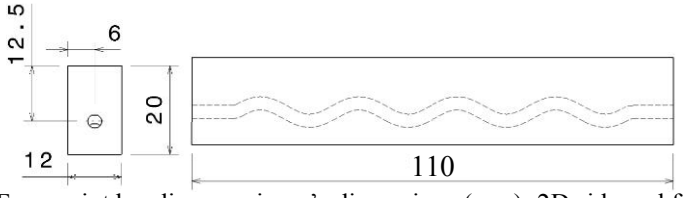

Figure 2: Four-point bending specimen's dimensions (mm): 2D side and front views

Table 1: LMD AISI 316L mechanical properties

σ_{yield} (MPa)	σ_{UTS} (MPa)	ε (%)	$E_{tension}$(GPa)
280 ± 10	567 ± 13	62 ± 5	163 ± 30

Table 2: SLM Ti6Al4V mechanical properties

σ_{yield} (MPa)	σ_{UTS} (MPa)	ε (%)	$E_{tension}$(GPa)
826 ± 17.2	964	12.84	107.71 ± 1.47

2.2 Test Procedure

The specimens were subjected to a cyclic fatigue loading with constant amplitude. A schematic of the four-point bending fatigue test is depicted in Figure 3. The locations with the highest probability for crack initiation from the capillary are situated at those cross-sections of the capillary that are furthest away from the neutral axis. The principal reason for this higher probability is directly related to the higher stress concentration at these locations. According to the step method the initial stress amplitude is chosen below the fatigue limit of the specimen. For each step a large number of cycles N with the same loading are applied. If failure did not occur the stress amplitude is increased with a selected step and again N numbers of cycles are applied [7]. This procedure is repeated until failure occurs. Since no previous results were available for the endurance limit of the additively manufactured AISI 316L and Ti6Al4V studied in this paper a conservative stress starting point was chosen.

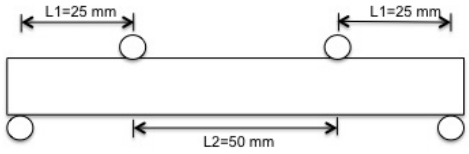

Figure 3: Schematic four-point bending setup

The fatigue tests were carried out on an MTS machine with a maximum static and dynamic load capability of 100kN. The applied sinusoidal cyclic load in each step had constant amplitude with an R ratio equal to 0.1 and frequency of 5Hz for SS316L (LMD) and 15Hz for Ti6Al4V (SLM). During the tests the specimen pressure transducer, the actuator load and displacement were monitored and registered by the controller of the MTS machine.

The specimens were equipped with a pressure transducer (Kulite XTL-123C-190M- 1, 7-BAR-A) at one side and with a check valve (Clippard MCV-1-M5) at the other side. After sealing, each specimen was placed in a vacuum chamber until the air in the capillary reached an absolute pressure of 0.55 bar. As a final step an extra stop (Clippard 11755-M5-PKG) was installed on the check valve as an extra occlusion. The final test specimen assembly is shown in Figure 4. In order to analyse the influence of the structural health monitoring on the micro-crack initiation, the fracture surfaces obtained after the fatigue tests were analysed with a scanning electrode microscope.

Figure 4: Final test specimen

3. RESULTS

3.1 Effective structural health monitoring during fatigue test

The first specimen of LMD AISI 316L has been subjected to nine steps, which corresponds to a total of 1.309.009 loading cycles for the first specimen before the crack penetrated the capillary and the test was automatically stopped. For each step 100.000 cycles were tested with the exception of step 8 and 9 where respectively 500.000 and 109.009 cycles were applied. The peak stress started from 9.9% of σ_{UTS} (56MPa) and reached 68.9% of σ_{UTS} (391MPa) in step 9 (see Table 3).

For the last specimen of LMD AISI 316L, in total 983.185 cycles within 4 steps were applied. The starting stress level was set at 79% of σ_{UTS} (446MPa) with 100.000 cycles per step. At the stress level of 89% of σ_{UTS} (502MPa) the number of cycles was increased to 500.000 cycles. The failure occurred according to the eSHM system after 283.185 cycles at 93.5% of σ_{UTS} (530MPa) in Step 4 (Table 3).

For the initial step of the first specimen of SLM Ti6Al4V the cyclic peak stress was limited to 25 % of σ_y and the number of cycles per step to 500.000. In subsequent steps the peak stress was increased by 10% of σ_y until the fatigue load reached the value of 71% of σ_y, where the crack was detected by the eSHM system. Twelve steps were tested for the first specimen. This gave a total of 5.514.591 loading cycles before the crack reached the capillary and the test was automatically stopped. For each step 500.000 cycles were tested with the exception of step 12 where 14.591 cycles were applied until the failure. The peak stress started from the 21,5 % of σ_{UTS} (207 MPa) and reached 69 % of σ_{UTS} (590 MPa) in step 12 (Table 3).

Regarding the last specimen of SLM Ti6Al4V the peak stress was increased by 10% of σ_y until the fatigue load reached the value of 69% of σ_y, where the crack was detected by the eSHM system. Six steps were tested, this gave a total of 2.752.000 loading cycles before a crack between the capillary and the outer surface of the part is formed. For each step 500.000 cycles were tested with the exception of step 6 where 252.000 cycles were applied until the failure, reaching 69 % of σ_{UTS} (570 MPa-Table 3).

Table 3: Overview of the different steps and stress levels for the LMD and SLM specimens

Specimen	Total Steps	Stress Level at Failure	Cycles at last step
LMD AISI 316L 1	9	391 MPa	109.009
LMD AISI 316L 2	4	530 MPa	283.185
SLM Ti6Al4V 1	12	590 MPa	14.591
SLM Ti6Al4V 2	6	570 MPa	252.000

During the tests at specified intervals and specifically at the last 10 completed loading cycles the absolute pressure level has been registered before the final failure. The absolute pressure increases stepwise when the crack penetrates the capillary. The varying character of the pressure increase is linked with the cyclic loading and the fact that the crack opens and closes during each load cycle. This phenomenon could be clearly observed by plotting the pressure values vs elapsed time for the last applied load cycles (see Figure 5(a), (b), (c) and (d)). For all the specimens the pre-set limit was 0.75 bar except the second specimen of LMD AISI 316L, where the pre-set limit was set to be 0.65 bar. On the moment that the pressure exceeded this value the actuator was switched off automatically. It is worth to mention that there is a difference in pressure behaviour between graphs (a), (b) and (d) with the graph (c) of the specimens. Currently, there is no clear explanation on this difference and further investigation needs to be done.

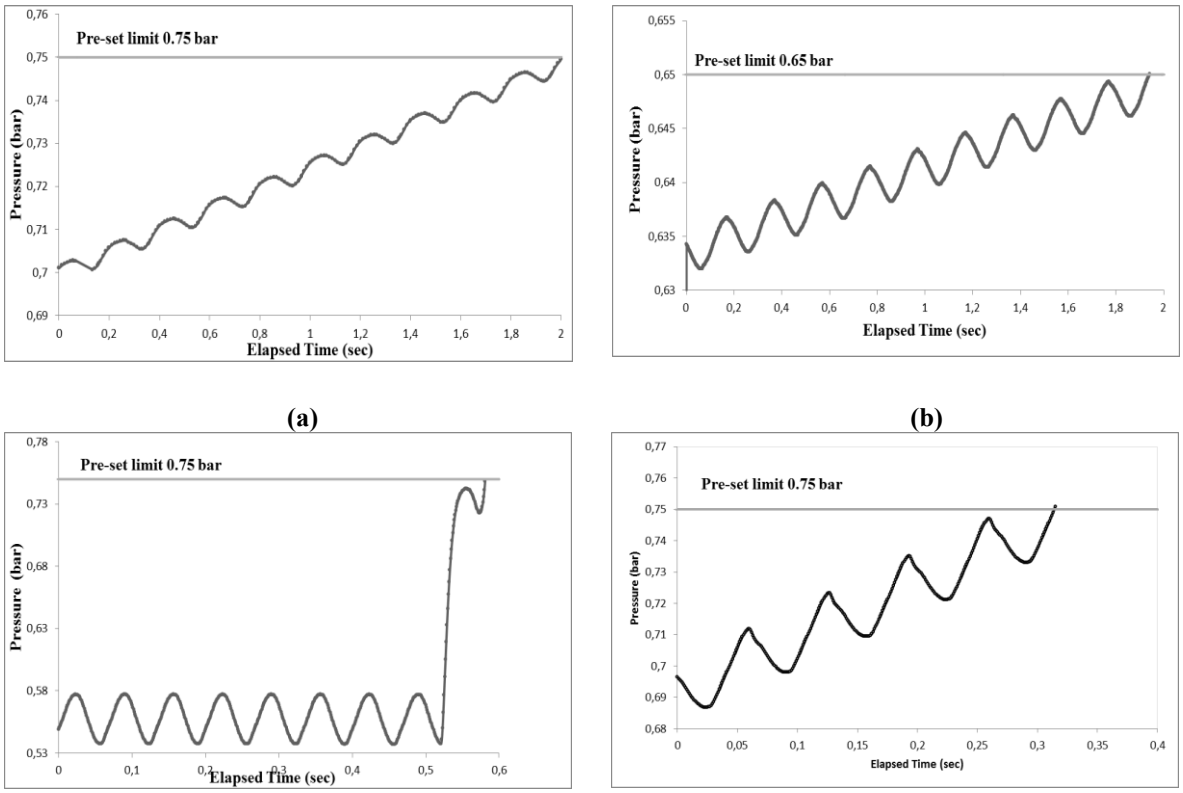

Figure 5: Pressure vs elapsed time for (a) the first AISI316L (LMD), (b) the second AISI 316L, (c) the first SLM Ti6Al4V and (d) the second SLM Ti6Al4V samples during the last load cycles

3.2 Fractographic analysis of the specimens after fatigue tests

According the ASM handbook of Fractography, a fracture surface is a detailed record of the failure history of the part. It contains evidence of loading history, environmental effects, and material quality[11]. Fracture analysis confirmed for the first specimen of LMD AISI 316L that the crack initiated from the outer surface towards the capillary (Figure 6 (a)). At the crack initiation locations oxide inclusions were detected on the fracture surface (Figure 6(a)). SEM-EDX analysis indicated that the oxide was rich in silicon, chromium and manganese. Fractography shows also that no cracks have initiated at the capillary (Figure 6(a)).

Alam et al. [12] demonstrated that close-to-surface pores and oxide inclusions are critical stress raisers and can initiate fatigue cracking having a severe effect on the fatigue life of structural components. For the first specimens of SLM Ti6Al4V (Figure 6(b)) the fracture surface is quite faceted and does not exhibit fatigue striations. The fractographic pictures reveal that the crack has initiated at the capillary region. A close-up of the initiation area is showing high concentrated porosity next to the capillary region (Figure 6(b)). Pores in the interior of the part could be observed on the fracture surface but they did not affect the crack initiation or propagation.

It can be concluded that high local porosity is an essential parameter for the effectiveness of the eSHM system. Fracture analysis has proven that the capillary has no impact on the crack initiation. However porosity is the main reason for crack initiation. It is of high importance to mention that the fracture surface could not be analysed on the second SLM Ti6Al4V specimen and the second LMD AISI 316L specimen. This is due to the fact that the eSHM system detected the crack but the location of the crack was not clear. As a result, further investigation of these samples is still needed.

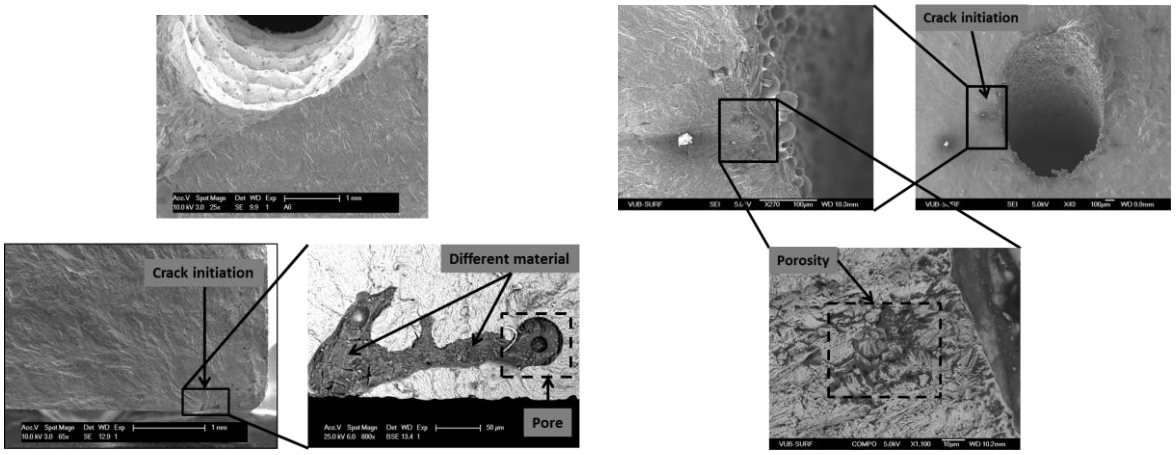

(a) **(b)**

Figure 6: Scanning electron microscope image of the fracture surfaces of the (a) LMD AISI 316L 1 and (b) SLM Ti6Al4V 1 specimens after the fatigue tests

CONCLUSION

All the tests were successfully stopped by the eSHM system that indicated the presence of a crack. During fatigue, the crack initiates due to porosity or oxide inclusions. This is evidence that concentrated porosity on additive manufacturing materials is the most essential parameter for crack initiation and further investigation is required. Fracture analysis is proving that the integrated SHM system had no influence on the crack initiation location for this four-point bending test setup and specimen. It can be concluded that the study and the experiments constitute the "proof-of-concept" validation of this application. As a result, the objective of this study, reaching the technological readiness level 3, has been proven.

ACKNOWLEDGEMENT

Research funded by an SBO Project grant 110070: eSHM with AM of the Agency for Innovation by Science and Technology (IWT).

REFERENCES

[1] C. R. Farrar and K. Worden, "An introduction to structural health monitoring.," *Philos. Trans. A. Math. Phys. Eng. Sci.*, vol. 365, no. 1851, pp. 303–15, Feb. 2007.

[2] D. Roach and S. NEIDIGK, "Does the maturity of Structural Health Monitoring technology match user readiness?," in *Proceedings of 8th International Workshop on Structural Health Monitoring*, 2011.

[3] ASTM Standard F2792 - 12a: "Standard Terminology for Additive Manufacturing Technologies", ASTM International, West Conshohocken, PA, 2003, DOI: 10.1520/C0033-03, www.astm.org.

[4] I. Gibson D. W. Rosen B. Stucker, *Additive Manufacturing Technologies*, vol. 76, no. 12. Springer, 2010.

[5] G. N. Levy, R. Schindel, and J. P. Kruth, "Rapid manufacturing and rapid tooling with Layer Manufacturing (LM) technologies, state of the art and future perspectives," *CIRP Ann. - Manuf. Technol.*, vol. 52, no. 2, pp. 589–609, Jan. 2003.

[6] J. P. Kruth, L. Froyen, J. Van Vaerenbergh, P. Mercelis, M. Rombouts, and B. Lauwers, "Selective laser melting of iron-based powder," *J. Mater. Process. Technol.*, vol. 149, no. 1–3, pp. 616–622, Jun. 2004.

[7] L. Sexton, S. Lavin, G. Byrne, and a. Kennedy, "Laser cladding of aerospace materials," *J. Mater. Process. Technol.*, vol. 122, no. 1, pp. 63–68, Mar. 2002.

[8] J. Schijve, "Fatigue of structures and materials in the 20th century and the state of the art," *Int. J. Fatigue*, vol. 25, no. 8, pp. 679–702, Aug. 2003.

[9] R. Bellows, S. Muju, and T. Nicholas, "Validation of the step test method for generating Haigh diagrams for Ti–6Al–4V," *Int. J. Fatigue*, vol. 21, pp. 687–697, 1999.

[10] D. A. Wanhill RJH, de Graaf EAB, "Significance of a rotor blade failure for fleet operation, inspection, maintenance, design and certification," *Fifth Eur. Rotorcr. powered lift Aircr. forum*, 1979.

[11] J. R. Mills, Kathleen Davis, "ASM Handbook," *ASM Int.*, vol. 12-Fractog, 1987.

[12] M. M. Alam, J. Powell, a. F. H. Kaplan, J. Tuominen, P. Vuoristo, J. Miettinen, J. Poutala, J. Näkki, J. Junkala, and T. Peltola, "Surface pore initiated fatigue failure in laser clad components," *J. Laser Appl.*, vol. 25, no. 3, p. 032004, 2013.